# Wind-Shear System Cost-Benefit Analysis

**Robert G. Hallowell and John Y. N. Cho**

Mitigating thunderstorm wind-shear threats for aircraft near the ground has been an important issue since the 1970s, when several fatal commercial aviation accidents were attributed to wind shear. Updating the knowledge base for airport wind-shear exposure and effectiveness of detection systems has become critical to the Federal Aviation Administration as they consider options for aging systems and evaluations of new systems.

**A series of fatal commercial aviation** accidents starting in the 1970s led to the identification of thunderstorm-related wind shear as a critical hazard to aircraft takeoffs and landings. In aggregate, these accidents resulted in over 400 fatalities and pressured the Federal Aviation Administration (FAA) to develop effective warning technologies. In response, the aviation community invested in and deployed wind-shear protection systems, ranging from pilot training for avoidance and recovery to sophisticated Doppler-radar detection algorithms for wind-shear warnings and detections.

This intense research effort led directly to the creation of Lincoln Laboratory's Weather Sensing Group, and the aggressive development and implementation program that followed resulted in the operational deployment of the Terminal Doppler Weather Radar (TDWR) at 46 airports during the 1990s and a Weather Systems Processor (WSP) modification for 35 existing Airport Surveillance Radars (ASR-9). In parallel, other organizations made improvements to the existing Low-Level Wind-Shear Alert System (LLWAS) for smaller airports. To date, there has not been a wind-shear-related accident at an airport that operates one of these modern wind-shear detection systems. The safety improvement was driven not only by the deployment of ground-based systems but also by improved pilot awareness and airborne onboard forward-looking radars (Predictive Wind-Shear System, or PWS). In addition, deployment of ground-based systems with automated alerts and associated training have enhanced air traffic controllers' awareness of wind shear and greatly improved their ability to provide pilots with proactive advisories of hazardous conditions.

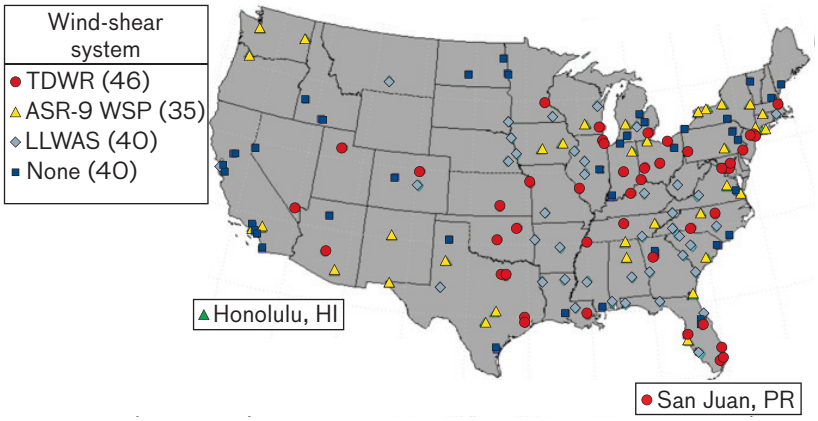


**FIGURE 1.** The airports considered in this study were distributed throughout the United States. The symbols indicate the wind-shear protection system currently operating at each airport. Note that nine of the Terminal Doppler Weather Radar (TDWR) airports are also equipped with an integrated network expansion Low-Level Wind-Shear Alert System (LLWAS).

an updated wind-shear exposure estimate for every airport in the National Airspace System (NAS) on the basis of the measured wind-shear activity from deployed systems, and a systemic model-based estimate of the expected effectiveness of ground-based wind-shear detection systems. The evaluation was performed for all of the 121 U.S. major airports that have some type of operational, ground-based wind-shear protection system and for an additional 40 feeder airports that are currently not protected by ground-based wind-shear systems. The locations and available ground-based protection are shown in Figure 1.

However, it has now been more than two decades since the first prototype radar tested the ability of Doppler-radars to detect wind shear, and more than a decade since the first TDWR became operational. While there has been a demonstrable decrease in the number and severity of wind shear and other weather-related accidents, there are substantial costs associated with operating and maintaining TDWR, WSP, and LLWAS. In addition to recurring costs associated with site- and second-level engineering support, significant nonrecurring costs accrue from hardware, processor, and software upgrades that are necessary to ensure long-term operational availability. For example, the FAA is currently executing a multiyear Service Life Extension Program (SLEP) for TDWR that addresses many of its major subsystems, including the antenna drive mechanism, signal and data processing computers, and user displays. Recently, new wind-shear detection technology has been developed, such as commercial lidar and X-band radar systems that might be useful in complementing or replacing the deployed systems.

Lincoln Laboratory was tasked with re-examining wind-shear system cost benefits in order to retrospectively evaluate the expected safety benefits of wind-shear mitigation measures and to provide a basis for evaluating future FAA wind-shear investment decisions. This work included a comprehensive analysis of the impact of evolving wind-shear protection on the wind-shear-related accident rate,

### Wind-Shear-Related Accidents

The National Transportation Safety Board (NTSB) is an independent agency responsible for the investigation of aviation accidents. The NTSB attempts to determine the cause of each accident logged, and detailed investigations are required for accidents involving serious or fatal injuries and/or major damage to aircraft. In the years 1975 to 2006, the NTSB attributed wind shear as the cause of 20 aircraft accidents, with a total of over 500 fatalities. Figure 2 shows the timeline of accident occurrences from 1975 to the present for all three aircraft categories. There has clearly been a marked decrease in the occurrence of wind-shear-related accidents even while total operations continue to increase.

One of the challenges in measuring the benefits of wind-shear-mitigation systems is that the frequency of

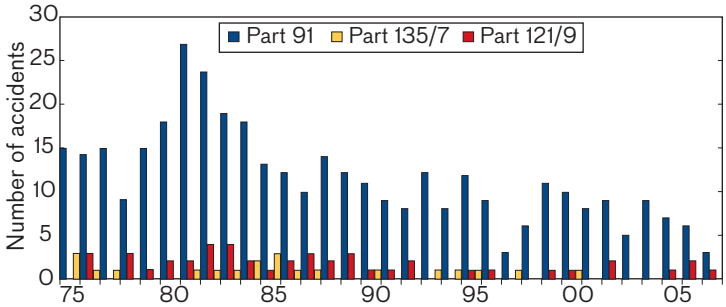


**FIGURE 2.** The timeline of wind-shear-related accident occurrences from 1975 through 2007 shows an improvement in all aircraft classes. Part 91 aircraft are general aviation aircraft, part 135/7 aircraft are air taxis, and part 121/9 aircraft are air carriers.

aviation accidents is very small compared to the total operations. In addition, reliable records of wind-shear-related accidents were available only a short time before mitigation techniques started to be employed, as shown in Figure 3. The bottom of Figure 3 illustrates a second factor that complicates matters—the implementation of various mitigation techniques has been ongoing since the early 1980s. Therefore, the NTSB data were used to calculate several accident-rate measures. The *baseline* is an estimate of the rate of wind-shear-related accidents prior to both the widespread awareness of pilots and the deployment of automated wind-shear protection systems. The *transitional* accident rate estimates the rate of wind-shear-related accidents as pilot awareness was rapidly increasing and initial LLWAS systems were being deployed but prior to the deployment of widespread automated radar-based wind-shear protection systems. The *protected* accident rate estimates the rate of accidents that have been occurring since the deployment of all current wind-shear protection systems (LLWAS, PWS, TDWR, and WSP). All of these measures are important in both estimating the benefits of wind-shear protection systems and helping to cross-check the estimated effectiveness of wind-shear mitigation measures.

### Wind-Shear Exposure Factor

Knowing an airport's exposure to wind-shear activity is a key factor in determining the relative accident risk at each airport. Hazardous wind shear comes primarily from microbursts that are caused by strong downdrafts in thunderstorms. The generated outflows typically range from 15 to 45 knots, but have been known to exceed 100 knots. An aircraft crossing a microburst, with its changing wind direction and shifting wind speeds, can induce a severe reduction in lift for the aircraft very near the ground. However, the leading edge of thunderstorm outflows typically occurring many kilometers ahead of an approaching thunderstorm can also be troublesome. The aviation safety

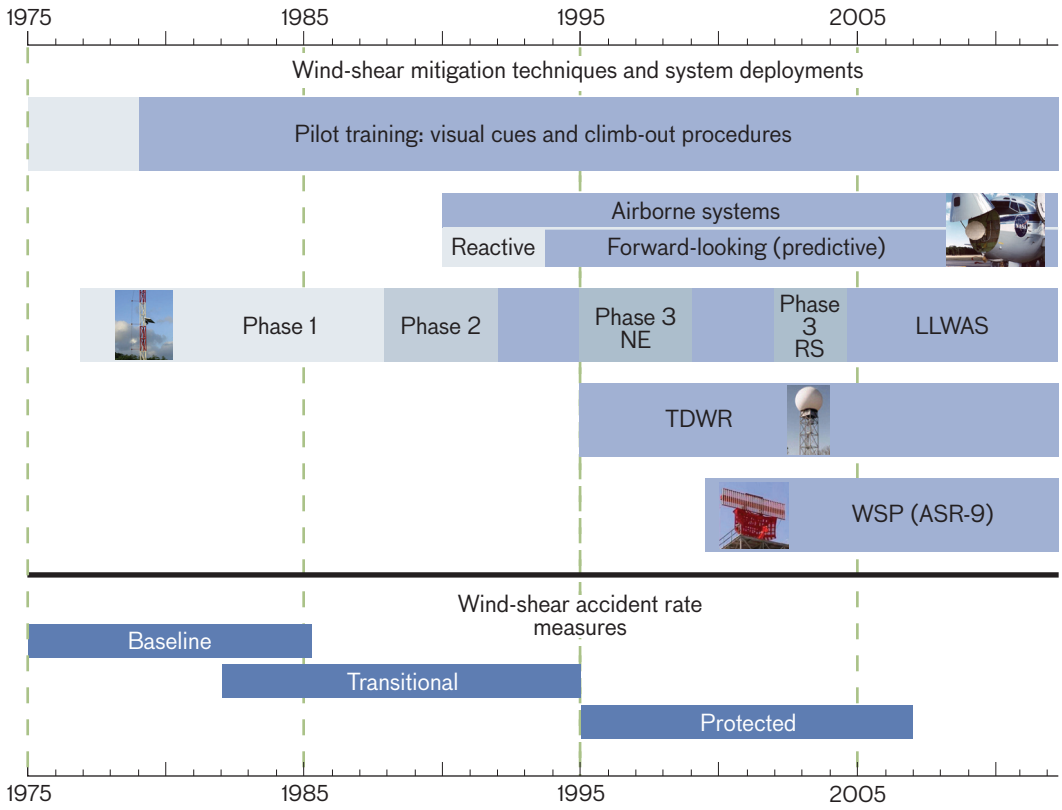


**FIGURE 3.** Wind-shear mitigation techniques and alerting systems have ramped up over time, covering more airports and aircraft with increasing levels of protection since 1975. Thus, defining the benefits of individual systems on the basis of accident-rate data is challenging since the baseline is being modified as time progresses. Dividing the history into baseline, transitional, and protected regions helps to constrain the benefits analysis.

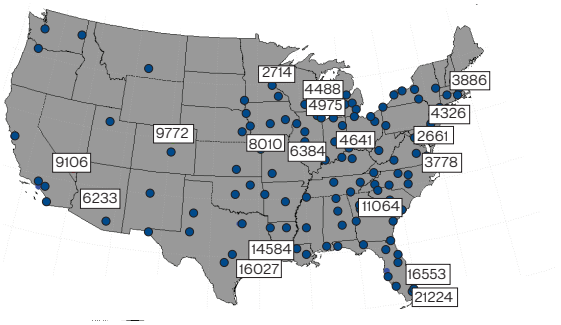


**FIGURE 4.** The values indicated are the actual measured number of minutes per year when at least one microburst was within 30 km radius of the respective TDWR/ITWS archive sites.

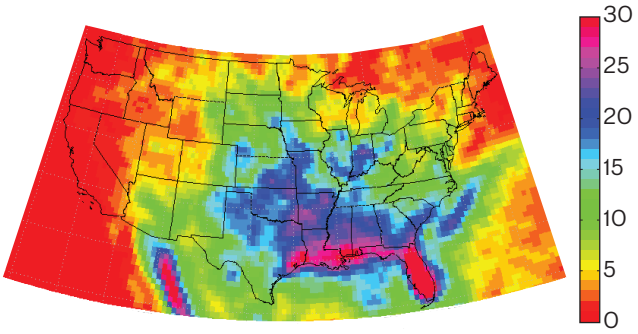


**FIGURE 5.** The NASA analysis of ten years of lightning flash-rate climatology (flashes/km$^2$/year) gives a clear indication of the primary locations of thunderstorms that produce wind shear.

hazard comes from the roll of winds at the leading edge of the outflow. Typically weaker, these *gustfronts* are more likely to be a problem for smaller aircraft [1].

TDWR microburst archived data report the exact location and strength for each alert shape—the warning regions in which wind shift is considered hazardous—generated by the TDWR system. The number of minutes that each site reported at least one microburst alert was chosen as the basis for wind-shear exposure risk. Archived data, however, were only available for one year at about 20 sites because the FAA does not routinely archive all sites. Figure 4 shows the archived data for a representative 18 sites. This snapshot of microburst activity needs to be interpolated over the entire country and at the same time needs to account for climatology of year-to-year variations.

There are two types of microbursts: wet and dry. Wet microbursts are generated by precipitation caught in the updraft of the thunderstorm that eventually collapses to the surface. Dry microbursts are driven by the evaporative cooling of relatively small amounts of water aloft in regions of large vertical temperature lapse rates. A ten-year climatology of average annual lightning flash rates over the United States provided a well-measured surrogate of thunderstorm activity to capture wet microbursts. Figure 5 shows the distribution of annual lightning flash-rate intensity over the contiguous United States while Figure 6 shows the comparison of lightning flash rates to microburst minutes for all of the archived sites. In addition, cloud base height, shown in Figure 7, or the height at which clouds typically begin to form, correlates to wind-shear activity; elevated heights enhance dry microburst activity [2].

All of these data on wind-shear rates were fit via a least-squares fit and the resultant wind-shear exposure formula is

$$MB = -0.7L^3 + 52.7L^2 - 726L + F(19.6C + 499.5) \qquad (1)$$

where $MB$ is the annual exposure to microbursts; $L$ is the lightning flash rate; $F$ is a low-lightning flash-rate factor (capped at 1.0); and $C$ is the average summer ceiling height in meters. Not unexpectedly, the most important factor in wind-shear exposure is the density of the lightning flash rate, with the secondary factor of ceiling height being especially important in the high plains region where dry microbursts dominate [3]. Regions with very low lightning flash rates (< 1.0 flash/minute) have very limited wind-shear activity (the Pacific Coast region, for example), and the model suppresses activity in these regions.

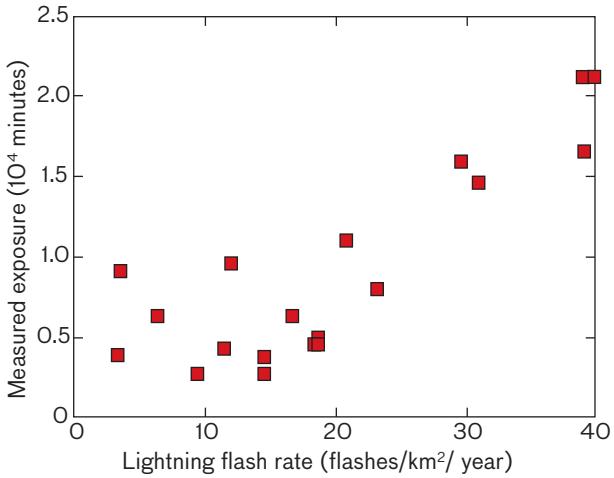


**FIGURE 6.** Microburst minutes correlate to annual lightning flash rates. Lightning activity thus provides a good indicator of the location of potential microbursts.

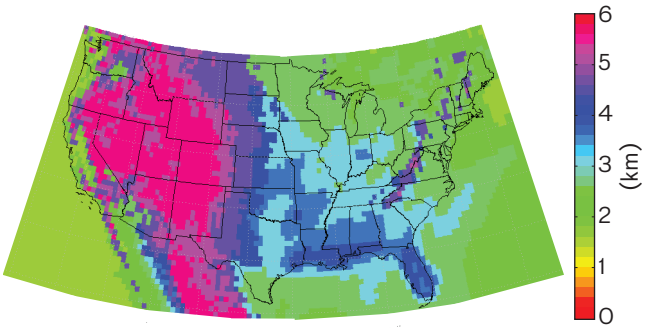


**FIGURE 7.** The average summer ceiling height (kilometers above sea level) is an additional indicator of microburst activity. The raw data were gathered from a 20-year data set of hourly station observations and are interpolated to a grid by fitting to lightning and terrain data.

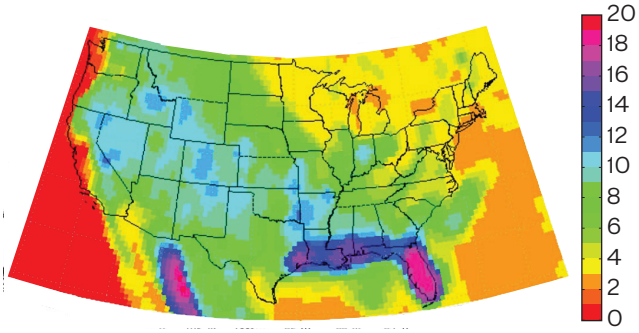


**FIGURE 9.** Note the similarity of the annual microburst exposure (based on station archive models) in this figure to the lightning flash rate in Figure 4 and secondarily to the cloud ceiling height shown in Figure 6. The scale is in thousands of minutes.

Figure 8 shows a map of the dry/wet tendency overlaid on a map of the United States based on historical precipitation data. Dry sites are mostly in the high plains, while wet sites are predominantly in the Gulf of Mexico and southeastern United States. A map of the interpolated microburst exposure over the entire United States is shown in Figure 9. Note the exponentially higher levels of microburst activity in the Gulf region and the strong drop-off in the Northeast and upper Midwest. A similar methodology was used to calculate the exposure to gust-fronts (not shown).

## Wind-Shear Mitigation Techniques

Consideration of mitigation techniques requires an evaluation of the probable improvement in wind-shear avoidance when an activity is applied. Safety benefits of applying a specific mitigation technique must focus on the reduction in accident probability of that technique. Such a reduction can be described as

$$P_{\text{Accident}} = (1 - P_{\text{Visual}}) \times (1 - P_{\text{Airborne}}) \times (1 - P_{\text{Ground}}) \quad (2)$$

where $P_{\text{Visual}}$ is the probability that a pilot will visually recognize and avoid an area of wind shear, $P_{\text{Airborne}}$ is the probability that an airborne system will detect and warn for wind shear, and $P_{\text{Ground}}$ the probability that a ground-based system will detect and warn for wind shear.

Each of the three potential mitigating detection techniques has its own advantages and disadvantages as well as cost-effectiveness. On clear days, viewing of disturbances or potential microbursts may be very effective, but the pilots may encounter cloud cover or they may be flying at night. Airborne and ground-based Doppler sensors are better at detecting wind patterns, but they are more expensive. Of course, one final factor to consider in avoiding dangerous wind shear is early detection—does the aircraft have sufficient time during the critical takeoff and landing sequences to avoid the effects of the weather?

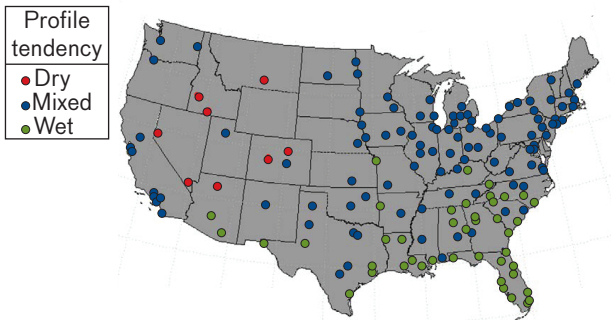


**FIGURE 8.** Weather conditions predominate what type of microburst activity occurs at each site. Dry microbursts occur more often in the high plains region, while wet microbursts occur most often in the Southeast and South.

### Modeling Pilot-Training Impacts

After the 1975 Eastern Airlines crash in New York was attributed to a microburst, pilots were trained in ways to recognize, avoid, and recover from wind-shear encounters. The FAA's wind-shear training-aid program started in 1987, and it stresses recognition and avoidance of wind-shear hazards. Pilots are told to look for visual clues such as virga (elevated rain shafts), plumes of dust and debris at the surface, and intense rain shafts that could all be indicative of microburst activity. Awareness is always heightened any time thunderstorms are present in the airport region.

Once these visual clues are seen, pilots are instructed to avoid the area under and around such features. However, in the event that the pilot enters the outflow, the FAA has defined specific criteria for maneuvering up and out of the hazard. So, there are three parts to the impact of pilot training: How visible are the visual clues that the pilot must see? How effective will a pilot be at recognizing the necessary features and avoiding the hazardous regions? And, what is the likelihood that the pilot can extract the aircraft if it nevertheless enters an outflow region?

Equation 3 illustrates an expression for the ability of pilots to see the visual microburst clues that they were trained to identify. Identifying visual microburst features is dependent on the event being during daylight/twilight hours and the ground being visible through clouds and precipitation. The time-of-day distribution of microbursts was based on an archive data set of microburst activity. From this data set, the percentage of time that microbursts actually occurred during daylight for a subsample of airports was determined and then interpolated over the whole country. The resultant distribution ranged from 71% daylight in Twin Falls, Idaho, to a peak of 83% in Fort Lauderdale, Florida. Figure 10 shows the estimated microburst daylight frequency breakdown across the continental United States.

Secondly, pilot observations can be restricted by the presence of clouds and precipitation that are blanketing the region around an airport. The region within 20 km of all studied airports was examined by utilizing a one-year archive of NEXRAD reflectivity data and a corresponding percent-visible field was calculated. If less than a third of the region had measurable reflectivity, it was assumed that the precipitation and clouds in the region would cover the airport region and a pilot would be capable of seeing most visual cues. High-reflectivity (wet) microburst environments typically have widespread precipitation coverage that makes it more difficult to see outflow events, while low-reflectivity (dry) environments have fewer meteorological obstructions. On average, wet environments are clear about 50% of the time, while dry environments are clear more than 85% of the time.

Finally, the human factor must be estimated—even if a pilot could see a hazardous outflow, would he recognize it as a hazard? There are very little hard data to generate this number. Even if we were to know how many outflows with visual clues were visible to a pilot, we have no way of tracking how many the pilot would actually recognize. Therefore, a flat estimate of 50% was used (as in the original TDWR study in 1994). Table 1 details the effectiveness factors for pilot observation at a subset of airport locations.

### Airborne Wind-Shear System Impacts

The Federal Acquisition Rule (FAR) 121.358, issued on 9 May 1990 [4], required that all air carriers (Part 121) aircraft be equipped with either a *reactive* wind-shear warning and flight guidance system or PWS radar. The reactive-system technology was developed in the mid-1980s by Boeing and Sperry and certified by the FAA in November 1985 as an enhancement to onboard Perfor-

$$V_{\text{Outflow}} = \%Daylight \quad (\%Dry \quad \%DryView + \%Wet \quad \%WetView) \tag{3}$$

$V_{\text{Outflow}}$ is the probability that the pilot can visually see outflow evidence,
$\%Daylight$ is the percentage of time that outflows occur during the daytime,
$\%Dry$ is the percentage of time that peak outflows are associated with reflectivities ≤ 20 dB,
$\%DryView$ is the percentage of time that dry outflows are unobscured by cloud cover,
$\%Wet$ is the percentage of time that peak outflows are associated with reflectivities ≥ 20 dB,
$\%WetView$ is the percentage of time that wet outflows are unobscured by cloud cover.

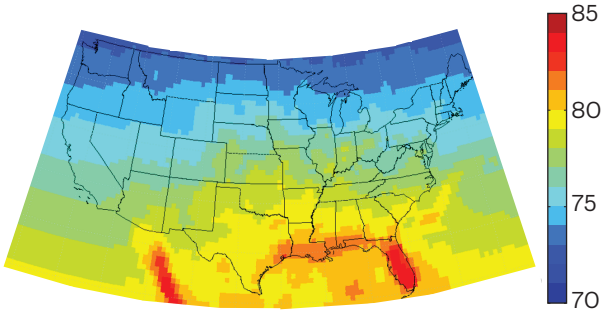


**FIGURE 10.** The estimated frequency of daylight microburst, *%Daylight* in Equation 3, activity again maps well to the lightning activity and cloud height of Figures 4 and 6. The scale is in percent.

mance Management Systems. Primary inputs are true airspeed, angle of attack, longitudinal acceleration, normal acceleration, and pitch. Performance was certified using computer models representing documented wind-shear conditions. The effectiveness probabilities that an aircraft equipped with a reactive system would recover from a wind-shear encounter without coming in contact with the ground are approximately 37.5 ± 12% [5]. But the raw accident rate that is used for the basis of this safety analysis already has the recovery of aircraft built into the analysis. Recovery is enhanced (to approximately 43.8 ± 15%), however, as new higher-performing aircraft are placed in service. The increase in recovery performance is taken into consideration when factoring airborne capabilities.

Predictive wind-shear warning systems were developed in the early 1990s by NASA Langley Research Center. Microwave radar, lidar, and passive infrared detection systems were evaluated through simulations and flight testing in conjunction with FAA prototype testing of TDWR in Denver, Colorado, and Orlando, Florida. The first microwave PWS radar was certified by FAA in September 1994, and today several systems are available for Part 121 aircraft (e.g., the Rockwell-Collins WXR-700 and the Honeywell RDR-4B). PWS radars compatible with regional-jet and general-aviation size constraints are not available at present.

The airline users we spoke with generally felt that the PWS radars were useful, but they uniformly emphasized that these were not a substitute for the ground-based systems. Broad-area situational awareness of wind shear—not attainable with the limited range of onboard systems—was felt to be essential for minimizing encounter risk.

The effectiveness of PWS radars has only been measured in simulated environments in which it often exceeds 95% effectiveness [5]. However, on the basis of the known limitations of the PWS in dry environments, effectiveness values are reduced because the distribution of outflows at each airport are associated with weak reflectivity.

## Modeling Ground-Based Wind-Shear Effectiveness

One of the key factors in estimating the benefits of a terminal wind-shear detection system is its performance. Thus, it is necessary to quantify the wind-shear detection effectiveness for each sensor, preferably on an airport-by-airport basis. To consider sensors that are not yet deployed, models must be developed that take into account the various effects that factor into the detection probability [6].

The sensors considered in this study are the existing FAA terminal wind-shear detection systems: LLWAS, TDWR, and the Airport Surveillance Radar Weather Systems Processor (ASR-9 WSP) [7–9]. We also included the National Weather Service Weather Surveillance Doppler-Radar (WSR-88D, more commonly known as NEXRAD) [10]. Furthermore, we included new sensors in addition to the currently deployed systems. The Lockheed Martin Coherent Technologies (LMCT) Wind Tracer Lidar is a commercially available product that has been field-tested at the Las Vegas, Nevada, airport (LAS) [11]. In addition, we have included a theoretical X-band radar replacement for the TDWR.

| AIRPORT | %DAYLIGHT | %DRY | %DRYVIEW | %WET | %WETVIEW | %HUMAN | %EFFECTIVENESS |
|---|---|---|---|---|---|---|---|
| BOS | 75 | 63 | 28 | 37 | 69 | 59 | 16 |
| ORD | 77 | 58 | 36 | 42 | 83 | 50 | 21 |
| LAS | 77 | 38 | 70 | 62 | 83 | 50 | 30 |
| MIA | 84 | 84 | 71 | 16 | 96 | 59 | 31 |

BOS - Boston, Massachusetts, ORD - Chicago, Illinois, LAS - Las Vegas, Nevada, MIA - Miami, Florida

**TABLE 1. Applying Equation 3 at several airports with varying wind-shear type (wet/dry) and activity provides an estimate of the effectiveness of pilot-only observation in wind-shear detection and avoidance. If pilots are trained to observe wind-shear indicators, they will be effective roughly 25 percent of the time.**

Table 2 shows which sensors already exist at which airports and which sensors are considered for new deployment at which airports. We did not consider the possibility of installing new TDWRs or ASR-9s because of prohibitive cost; new WSPs are only considered for already existing ASR-9s. Deploying new or moving existing NEXRADs was also not considered.

The detection coverage areas of interest, shown in Figure 11, were the union of the Areas Noted for Attention (ARENAs) for microbursts and an 18 km radius circle around the airport for gustfronts. An ARENA polygon consists of the runway length plus three nautical miles in the approach direction, two nautical miles in the departure direction, and one nautical mile width. The 18 km extent of the gustfront coverage corresponds to the distance a gustfront would travel at 15 m/s in 20 minutes, which is an appropriate metric for gustfront anticipation lead time in the context of airport operations. Gustfront detection is important for delay-reduction benefits. (The TDWR generates gustfront products out to 60 km from the airport.)

**Radar Performance Analysis**

Of the radar systems considered in this study, the TDWR has the best performance characteristics for terminal wind-shear detection—it has the highest weather sensitivity and the narrowest antenna beam (for clutter avoidance), and its use is fully dedicated to this mission. It also incurs the highest cost to the FAA because it is not shared with other agencies or missions and is located on its own site away from the airport. The WSP is a signal processing system that is piggybacked onto the ASR-9 terminal aircraft surveillance radar, so the incremental cost is quite low. However, being dependent on the vertical fan beam and rapid scanning rate of the ASR-9, it is far from an ideal system for low-level wind-shear detection. The NEXRAD is only slightly less sensitive to weather compared to the TDWR and has a 1° antenna beam, and its cost is shared by two other agencies besides the FAA. However, it is often not located close enough to the airport, and its volume scanning strategy, which is tailored to wide-area coverage, is too slow for microburst alerting.

| SENSOR | CURRENT AIRPORT CONFIGURATIONS | | | | | |
|---|---|---|---|---|---|---|
| | TDWR (46) | WSP (35) | LLWAS-RS (40) | OTHER (40) | DUAL-SENSOR COMBINATIONS | TRI-SENSOR COMBINATIONS |
| TDWR | Existing | N/A | N/A | Existing* | Lidar<br>LLWAS<br>NEXRAD | NEXRAD +Lidar<br>NEXRAD +LLWAS |
| WSP | New | Existing | N/A | Existing* | Lidar<br>LLWAS<br>NEXRAD | NEXRAD +Lidar<br>NEXRAD +LLWAS |
| LLWAS | Existing (9)<br>New (37) | New | Existing | New | | |
| NEXRAD | Existing* | Existing* | Existing* | Existing* | Lidar<br>LLWAS | |
| LMCT Lidar | New | New | New | New | | |
| LMCT X-band | New | New | New | New | Lidar<br>LLWAS | |

* Closest to airport

**TABLE 2.** The current configurations of the 161 airports in this study range from TDWR to airports with no local radar. The various additional configurations listed in the left column were analyzed to evaluate cost benefits. Adding TDWR or WSP to those airports that do not currently have the capability was not considered because of their prohibitive costs.

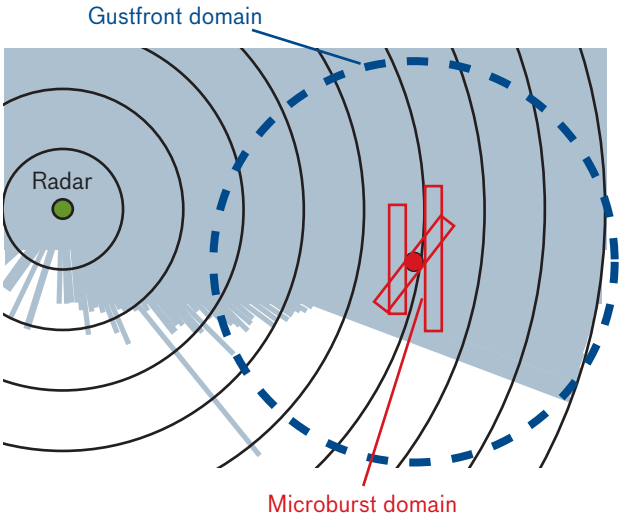


**FIGURE 11.** Radar coverage (the light blue regions) indicates where, within the microburst and gustfront domains, the radar will be effective. The dotted circle is an 18 km radius area of gustfront study. The red rectangles are the runway coverage areas analyzed for microbursts. The white regions are those areas that the radar does not cover (because of ground clutter or other limitations).

The proposed LMCT X-band radar should have performance and cost profiles that are somewhere in between the TDWR/NEXRAD and WSP extremes.

Table 3 shows some of the relevant system parameters and the minimum detectable dBZ at 50 km range for the four radars studied. Although the latter quantity does not include precipitation attenuation effects, the impact of attenuation was included in the X-band analysis since the impact on performance can be significant.

Radar signal detection can be noise limited or clutter limited. In the latter case, the clutter suppression capability determines the detection performance. All three existing radars (TDWR, NEXRAD, ASR-9), which have klystron transmitters, are undergoing or expected to undergo an upgrade that will bring the maximum possible clutter suppression to about 60 dB. The LMCT X-band radar has a magnetron transmitter with an expected maximum clutter suppression capability of 50 dB. The post-upgrade performance figures were used in the cost-benefit analysis.

The ability of a radar system to detect low-altitude wind shear depends not only on the radar sensitivity and clutter suppression capability, but also on viewing geometry, clutter environment, signal processing and detection-algorithm effectiveness, and the characteristics of the wind shear itself. Figure 12 shows some of the issues in radar detection of wind shear with real-world limitations. Thus, although the system characteristics may be invariant with respect to location, there are many site-specific factors that affect the probability of detection ($P_d$) performance. In this study, we tried to objectively account for as many of these factors as possible.

A high-level flow chart of the radar wind-shear $P_d$ performance estimator is shown in Figure 13. For each radar at a given site, a clutter residue map was generated by using digital terrain-elevation data, digital feature-analysis data, and radar characteristics. Probability distribution functions (PDFs) of the wind-shear reflectivity $P(Z_{ws})$ and outflow depth $P(h_{ws})$ were also generated for each radar at a given site. These were produced using a combination of wind-shear data collected during field experiments and modeling based on nationwide proxy parameters. The interest area, as explained previously, was the union of the ARENAs for the microburst case and an 18 km radius circle around the airport for the gustfront case.

With a range-azimuth grid centered on the radar, the minimum detectable reflectivity is computed for each cell inside the interest area. This calculation involves many factors, including system sensitivity, terrain blockage, clutter signal and the ability of the system to suppress it, range-alias contamination likelihood and the capacity of the signal processing to mitigate it, signal loss and clutter gain caused by partial beam filling, and attenuation from intervening precipitation. The probability of the wind-shear signal being visible above the noise and clutter in that cell is computed by integrating upward from the minimum detectable reflectivity over the wind-shear reflectivity PDF. The mean over all the cells in the interest area is then calculated with the result from each cell weighted by its area. This overall wind-shear visibility is then multiplied by the maximum success rate of the wind-shear detection algorithm (i.e., the best detection rate for a specified false-alarm rate that the algorithm can yield if given noise-free images of wind shear) to arrive at the estimate of wind-shear detection probability.

### Lidar

The LMCT Doppler lidar operates at a wavelength of 1.6 $\mu$m with an average transmitted power of 2 W. It has a laser beam diameter of 10 cm, a range resolution of 30 to 50 m, and a maximum scan rate of 20°/s [12].

| PARAMETER | TDWR | ASR-9 WSP | NEXRAD | LMCT X-BAND |
|---|---|---|---|---|
| Peak power (kW) | 250 | 1120 | 750 | 200 |
| Pulse length (ms) | 1.1 | 1.0 | 1.6 | 0.4 |
| Antenna gain (dB) | 50 | 34 | 45.5 | 43 |
| Beamwidth (degrees) (azimuth × elevation) | 0.55 × 0.55 | 1.4 × 4.8 | 0.925 × 0.925 | 1.4 × 1.4 |
| Wavelength (cm) | 5.4 | 11 | 10.5 | 3.3 |
| Maximum clutter suppression (dB) | 57 (60*) | 48 (60*) | 50 (60*) | 50 |
| Rotation rate (deg/s) | ~20 | 75 | ~20 | ~20 |
| Pulse-repetition frequency (Hz) | ~1600 | ~1100 | ~1000 | ~2500 |
| Minimum detectable dBZ at 50 km** | -11 | 7 | -10 | -3 |

* After upgrade
** Without precipitation attenuation

**TABLE 3.** Relevant radar system parameters for the four radars studied show their similarities and differences, including the minimum detectable signal strength (in dBZ) at 50 km range.

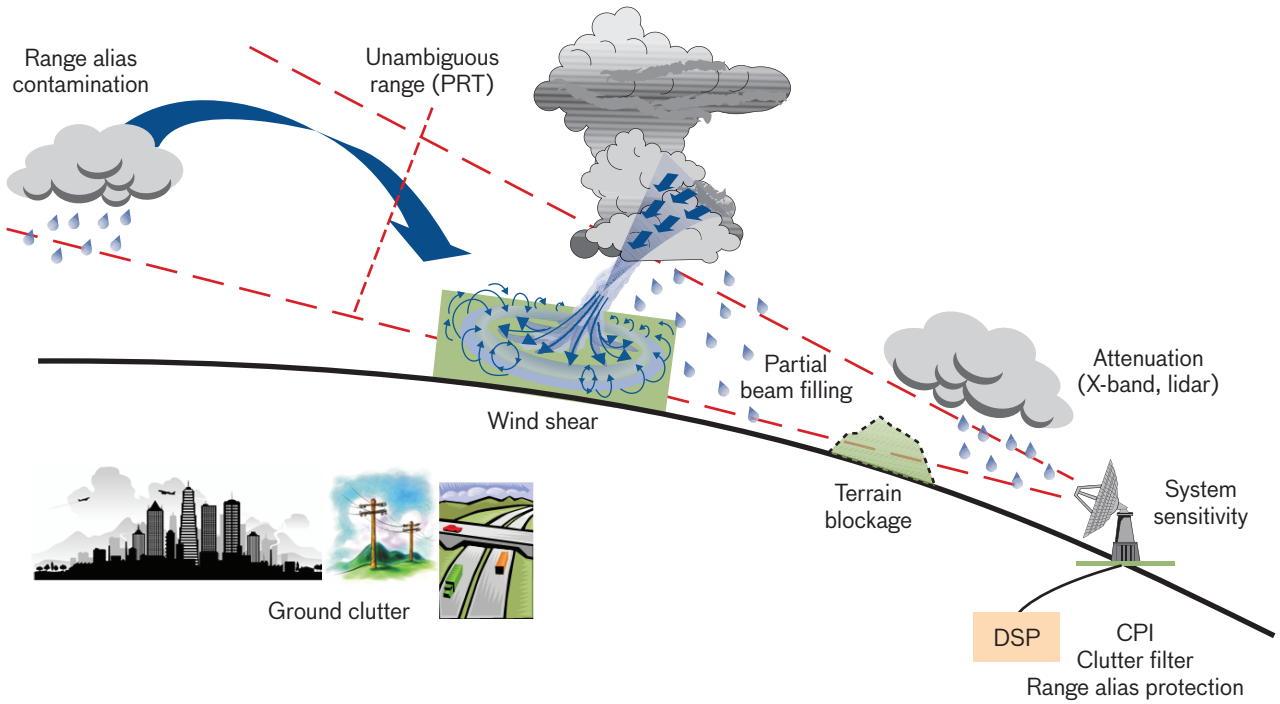


**FIGURE 12.** Those regions in Figure 11 that indicated areas that the radar did not cover are due in part to several issues. Ground clutter and terrain can block the radar entirely, while atmospheric conditions may attenuate or block the beam.

Lidars operate at much shorter wavelengths than radars, and the balance between scattering and attenuation relative to particles in the atmosphere is quite different. For a lidar, the maximum range occurs in the absence of large, attenuating precipitation particles and in the presence of aerosols that provide effective backscattering. The detection range generally decreases with increasing dBZ along the propagation path. Therefore, the integration over the wind-shear reflectivity PDF in computing the visibility should be computed downward from a maximum detectable reflectivity.

This is a simplified model of the actual physical process because dBZ is a radar-based quantity that corresponds well to the lidar attenuation but not the backscattering strength. For our analysis, we were only concerned with two specific meteorological situations—a microburst at close range and a gustfront approaching from a distance. On the basis of a sensitivity model that incorporated field testing data, LMCT provided us with maximum range versus dBZ curves for the microburst case and for the gustfront case at wet and dry sites.

Because the lidar beam is collimated, we assumed that it successfully avoids ground clutter altogether. (We did include terrain blockage for the 18 km radius around-the-airport gustfront case, assuming a beam elevation angle of 0.7°.) Thus, the detection probability estimation scheme, which follows the radar model, becomes much simpler because the clutter effects are removed. These characteristics of the lidar (maximum sensitivity at low dBZ and not being affected by clutter) make the lidar an ideal complement to a radar. As with the X-band radar, we assumed that it would be sited in the center of the union of the ARENAs on an 8 m tower.

## LLWAS

The LLWAS obtains its wind measurements from anemometers mounted on towers at multiple locations in the airport vicinity. The wind-shear detection coverage provided is therefore directly dependent on the distribution of the anemometers and is limited to a small area compared to the radars and lidar. The number of sensors per airport is 6 to 10 for the LLWAS-RS and 8 to 32 for the LLWAS-NE++ (network expansion).

The coverage provided at each LLWAS-equipped airport is given in the database as (nautical) miles final on arrival and departure for each runway. Since the ARENA is a one-mile-wide corridor from three miles final arrival to two miles final departure (runway inclusive), it is simple arithmetic to compute the LLWAS coverage from these numbers. The microburst detection probability is then estimated as the product of the coverage and the LLWAS detection algorithm detection probability, which we took to be 0.97 (for a false-alarm probability of 0.1) [13].

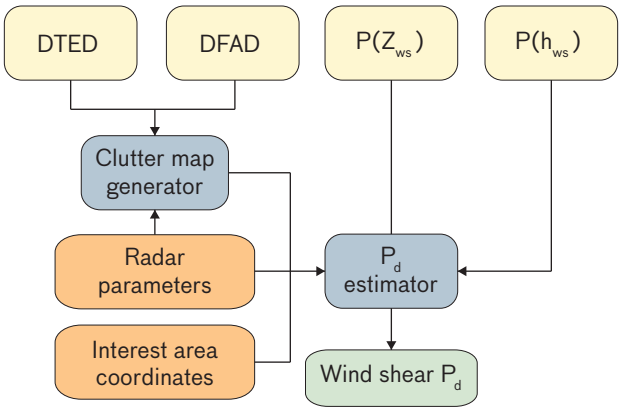


**FIGURE 13.** Calculating the wind-shear probability of detection ($P_d$) performance through this high-level flow chart provides a test of the quality of the $P_d$ estimator program. In this figure, DTED is the digital terrain-elevation data; DFAD is the digital feature-analysis data (e.g., roads, transmission lines); $P(Z)$ is the wind-shear reflectivity ; and $P(h)$ is the outflow depth.

## Sensor Combinations

Fusion of data from multiple sensors has the potential to increase wind-shear detection probability. At the minimum, holes in the coverage of one sensor that are due to blockage, clutter residue, or lack of sensitivity, for example, may be filled in by another sensor with better sensing conditions in those areas. Line-of-sight velocity fields cannot be directly merged for noncollocated sensors, but sophisticated detection algorithms that perform fuzzy-logic operations on interest fields would allow merging at that level instead of at the base data level. Therefore, for radar + radar and radar(s) + lidar combinations, we computed the visibility pixel by pixel for each sensor and took the greater value before summing over the interest area.

In the case of radar(s) + LLWAS, the detection phenomenologies are independent of each other. The data on which the detection algorithms work are quite different—volumetric base data for the radar and point measurements of surface winds for the LLWAS—so they cannot be

fused together in the same way as the radar and lidar data. In practice, the detection alert is issued after combining the wind-shear message outputs from the two systems [14]. Thus, we took the detection probability, $P_d$, for each sensor and combined them as $P_d$(combined) = 1 – [1 – $P_d$(radar)][1 – $P_d$(LLWAS)]. In theory, the false-alarm rates also combine to increase in similar fashion. However, clever use of all the available contextual data can reduce false alarms so we assumed that the false-alarm rate stayed constant.

## Methodology for Costs/Benefits Assessment

The time period used for all calculations is from 2010 to 2032; this time frame is primarily driven by the evaluation of potential alternatives. Current configurations of systems are assumed to continue from 2010 to 2012 and then alternative costs and benefits are figured for a twenty-year life-cycle (2013–2032). Some alternatives may take longer to implement than others, but the three-year assumption allows for similar cost comparisons between the various system combinations. Cost and benefits projections require that forecasted values be depreciated back to a constant dollar figure; in this case, we use fiscal year 2008 (FY08) constant dollars. Therefore, for both benefits and analysis figures, an FAA-recommended value of 7% is used for this depreciation [15]. Note that this is particularly important when it comes to costs of initial implementation, as these costs will be depreciated the least.

## Assessing Safety Benefits

The potential safety benefits for each airport and each category of aircraft for each ground wind-shear system configuration are based on five factors as shown in the equation below. Accident costs capture the expected societal and actual costs that are expected to occur if an aircraft crashes because of wind shear. Accident rates estimate the frequency with which accidents would occur, given that no ground-based wind-shear systems were present. Forecasted operations and enplanement rates used to predict future safety exposure are based on the number of aircraft and people at risk over the evaluation period (2010–2032). The Safety Weather Exposure Factor (SWEF) is a measure of the relative exposure of an airport's operations to wind shear. Finally, the change in system efficiency measures the difference between the current ground-based wind-shear detection system and each alternative (proposed earlier in Table 3).

| Potential safety benefits ($) | = | Accident costs ($) | × | Accident rates (accidents per operation) | × | Forecast operations and enplanements | × | Safety weather exposure factor (SWEF) | × | Change in system efficiency relative to baseline |
|---|---|---|---|---|---|---|---|---|---|---|

### Accident Costs

In the equation, accident costs are derived from values defined in FAA guidelines for economic analyses [16, 17]. To evaluate the cost of a typical wind-shear accident, we must estimate the accident cost "structure" on the basis of the breakdown of personal injury and infrastructure losses from previous wind-shear accidents. Utilizing the distribution of personal fatalities/injuries and infrastructure losses, the average safety costs associated with a wind-shear accident can be calculated. Table 4 lists the results for all accidents over the period from 1975 to 2007.

### Accident Rate Modeling

As detailed earlier, there are three eras of accident rates that were calculated: baseline (1975–85), transitional (1982–94), and protected (1995–2007). Each time period captures a different state of wind-shear mitigation; consequently, the models of pilot training, airborne systems, and ground-based systems can be used to transform accident rates between eras. Figure 14 illustrates this concept for Part 121/9 aircraft; the bars with hatching are the measured accident rates during the three time periods. By using models of the effectiveness of each wind-shear mitigation technique from pilot training and airborne systems to individual ground-based systems, each accident era can be "corrected" by either adding or subtracting the impact of various safety measures. For example, the red hatched bar for 1975–85 represents the measured accident rate for that time period. Correcting this accident rate for the pilot

| COSTS (2008$) | AIRCRAFT CATEGORY | | |
|---|---|---|---|
| | AIR CARRIER | AIR TAXI | GENERAL AVIATION |
| People | $ 117,345,503 | $5,086,966 | $ 1,714,929 |
| Aircraft | $ 4,922,000 | $ 1,626,108 | $ 148,620 |
| Total | $123,267,503 | $ 6,713,073 | $1,863,548 |

**TABLE 4.** The estimated average wind-shear-related accident costs are based on FAA guidelines that assign values to people (deaths and injuries) and aircraft (damaged or destroyed).

the total United States operations covered by the 161 study airports is roughly 94%, 59%, and 10% for air carrier, air taxi, and general-aviation (GA) operations, respectively. While a large portion of GA traffic and therefore total traffic are nonstudy airports, these GA operations are spread out over hundreds of small airports, and GA traffic is the most difficult class of aircraft to reach for wind-shear warnings. The disparity in the numbers of air carrier types is not unexpected because large airports with heavy aircraft are less desirable for small aircraft and recreational users.

training model gives the solid green bar under the heading With Pilot Training. Adding predictive wind-shear systems results in the yellow bar, and, finally, by adding the current ground-based constellation of TDWR, WSP, and LLWAS, one obtains the blue bar. Conversely, the measured "protected" accident rate from 1995–2007 can be corrected backwards to remove each mitigation technique.

This manipulation of the accident rates provides a better average estimate of the "unprotected" accident rate that can be used for all benefits calculations. Variability for air taxi (Part 135/7) and general-aviation (Part 91) aircraft is much larger than for Part 121/9 aircraft in part because the models for pilot training and estimates of impact on aircraft outside ground-based protection are more limited. Table 5 lists the pooled average accident rate and the range of values over the three corrected unprotected rates for each aircraft category.

### Forecasted Operations and Enplanements

The number of operations for each aircraft type and each airport are obtained from the FAA Terminal Area Forecasts [15]. Table 6 shows the number of operations (2008) for each class of wind-shear study airport and the remaining NAS traffic. Over 94% of the major air carrier traffic is covered by the study airports chosen, with almost 90% of the overall traffic protected by some active wind-shear system. The percentage of

### Safety Weather Exposure Factor

SWEF is used to weight the risk of each operation at individual airports in terms of exposure to wind shear. Wind-shear exposure for safety comes primarily from microburst outflows but some gustfronts are strong enough to cause additional concern. The SWEF number combines the two risks by weighting microburst exposure at 90% and gustfront exposure at 10%. Microburst exposure is determined by calculating the average microburst-related wind-shear exposure factor over all of the 161 airports being analyzed. An implicit assumption is made that the 161 airports are sufficiently dispersed that they represent the average exposure over the entire country.

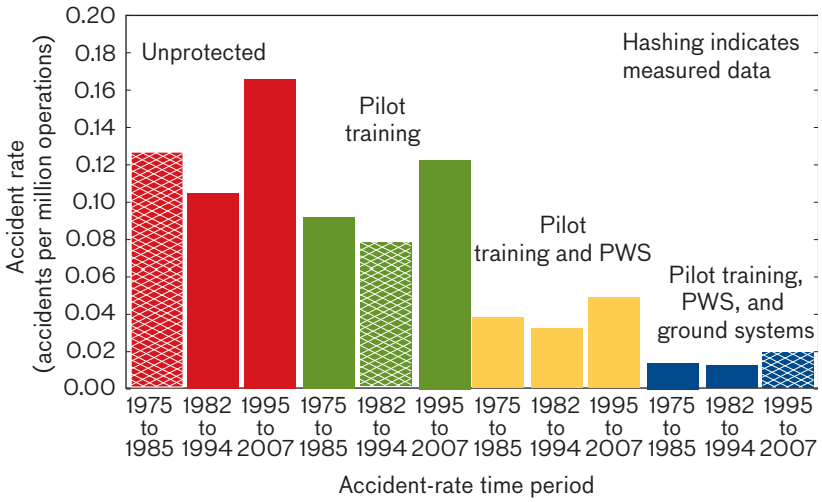


**FIGURE 14.** A comparison of measured and mitigation-adjusted accident rates permits the "filling out" of the entire chart. The bars with hatching are the measured accident rates. Modeling the other protection conditions from the measured data provides estimates of accident rates for all possible mitigations in each time period.

| AIRCRAFT CATEGORY | AVERAGE RATE | RANGE |
|---|---|---|
| Part 121/9 | 0.1095 | 0.1045–0.1168 |
| Part 135/7 | 0.2037 | 0.1299–0.2410 |
| Part 91 | 0.1600 | 0.1201–0.1842 |

**TABLE 5.** Baseline values, both observed and calculated, of the number of "unprotected" accidents are required to determine the cost benefits of mitigation techniques. Here, the average and range of wind-shear-related accident rates are listed by category of aircraft. The units are number of "unprotected" accidents per million operations.

The relative microburst exposure for each airport is then the airport exposure divided by the average. An exposure factor of 1.0, therefore, represents an airport risk that is exactly the average. If the ratio is higher (lower) than 1.0, then the exposure is higher (lower) than average. The same calculations are made for gustfront exposure and then the two values are combined together (90% microburst + 10% gustfront) to obtain the SWEF.

## Estimating System Costs

Both the currently implemented and alternative wind-shear systems evaluated in this report have operating and/or building costs associated with them. In assessing the relative value of wind-shear system value, one must reduce the overall benefit of the system by its associated cost. Therefore, each alternative was examined to estimate the cost of operating existing systems and implementing and then operating alternative systems and/or configurations.

Cost data were gathered by MCR Federal, Inc., using both actual cost data (for existing systems like TDWR, WSP and LLWAS) and estimated costs obtained from vendors and FAA staff for alternatives (X-band, NEXRAD, and lidar-based systems). Table 7 summarizes the average cost per system. Any technical refreshing or SLEP costs associated with the existing legacy systems (TDWR, WSP, and LLWAS) were included in the "in-service management" costs. Where applicable, these costs were included in the implementation costs for the newer systems. Figure 15 shows the comparison of life-cycle cost grouped by system type. Note that system costs are spread out over different numbers of sites, depending on the system installation.

## Current Airport-Specific Safety and Delay Mitigation

Several layers of wind-shear mitigation are in current use. This section details the current situation by examining (1) the assessment of the NAS completely unprotected for wind shear, (2) pilot training benefits, (3) airborne systems benefits, and (4) the current and near-term baseline ground-based benefits. Figure 16 shows the relative safety exposure based on the level of wind-shear protection that is applied. The red vertical bars show the variation in this exposure based on the estimated variability of accident rate estimates given in Table 5.

Results throughout this section are typically given as an overall total and an annual liability or benefit over the period 2010 to 2032, with charts showing the breakdown by current site configuration and individual airports where necessary. These values are given in current value fiscal year 2008 dollars. Therefore, annual figures correspond to the base year FY08 dollars that would represent the total current value if that cost occurred each year. Consequently, this figure is significantly higher than just dividing the total current value cost by the total number of years. Only

| AIRPORT SENSOR TYPE | AIR CARRIER | AIR TAXI | GENERAL AVIATION | TOTAL |
|---|---|---|---|---|
| TDWR | 9.3 | 5.4 | 1.5 | 16.2 |
| WSP | 2.2 | 1.5 | 1.8 | 5.5 |
| LLWAS | 1.1 | 0.9 | 3.2 | 5.2 |
| Non-study airports (unprotected) | 0.8 | 6.1 | 74.4 | 81.3 |
| Total | 14.1 | 14.8 | 82.7 | 111.6 |

**TABLE 6.** The breakdown of aircraft operations by airport type is clearly biased toward general aviation (smaller aircraft) at unprotected airports. Since it would be prohibitively expensive to allocate improved ground-based sensors at all these sites, they were not studied in this work. The units are millions of operations in 2008.

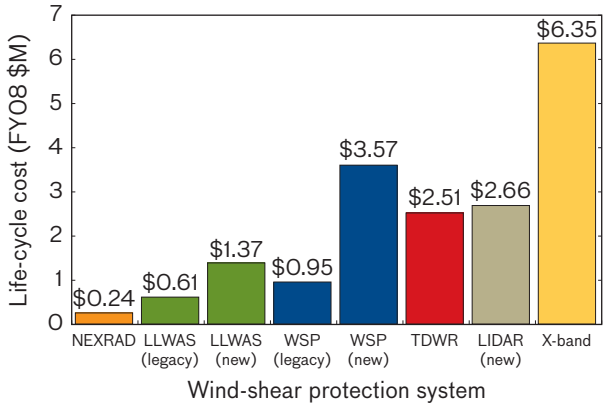


**FIGURE 15.** Total life-cycle (2010–2032) system costs per airport for wind-shear protection systems shown here should be compared to the expected benefits of mitigating accidents to determine the appropriate action at each airport. The following numbers indicate the number of potential sites, or costed systems, at which the protection system could be implemented: NEXRAD, 46; LLWAS legacy, 35; LLWAS new, 40; WSP legacy, 74; WSP new, 80; TDWR, 121; LIDAR new, 161; and X band, 161.

safety liability is discussed for items (1) through (3), while delay measures are considered for the current and near-term ground-based coverage. Alternative systems' benefit changes were modeled to begin in 2013; the existing benefits were assumed to stay in effect from 2010–2012.

### Pilot Training Assessment

Pilot training is the first mitigation technique and the effectiveness of this training is applied to all forms of air traffic equally (air carrier, air taxi, and general aviation). Therefore, it is the strategy with the most widespread impact. As shown in Figure 16, for the airports studied, the total safety exposure reduction because of pilot training is $728.7 million or 26% ($69.2 million annually). The rank order of sites changes only slightly as some airports have environments in which it is easier for pilots to identify visual cues. For example, Orlando, Florida, and Chicago, Illinois, swap places in the top-10 exposure list as Chicago O'Hare's pilot observability effectiveness is 21% but Orlando's is 29%.

| WIND SHEAR SYSTEM | ESTIMATED NUMBER OF COSTED SYSTEMS | ONE-TIME IMPLEMENTATION COSTS ($K) | LIFE-CYCLE IN-SERVICE MANAGEMENT COSTS ($K) | TOTAL COSTS (2008 BY $K) | TOTAL COSTS 2010–2032 (2008 PV $K) |
|---|---|---|---|---|---|
| Existing TDWR | 46 | N/A | $5009 | $5009 | $2507 |
| Existing WSP | 35 | N/A | $1953 | $1953 | $947 |
| Existing LLWAS | 40 | N/A | $1321 | $1321 | $605 |
| Existing NEXRAD (with updated algorithms and scanning) | 74 | $178 | $266 | $444 | $242 |
| New WSP | 80 | $4104 | $1255 | $5359 | $3574 |
| New LLWAS | 121 | $843 | $1698 | $2541 | $1355 |
| New lidar and algorithms | 161 | $2461 | $1979 | $4440 | $2656 |
| New X-band radar and algorithms | 161 | $7356 | $1972 | $9328 | $6350 |

**TABLE 7.** Total life-cycle (2010–2032) system costs per airport for wind-shear protection systems should be compared to the expected benefits to mitigating accidents to determine if there is a net benefit for the implementation of the system. Base Year (BY) costs are uncorrected while Present Value (PV) depreciates future dollars for inflation.

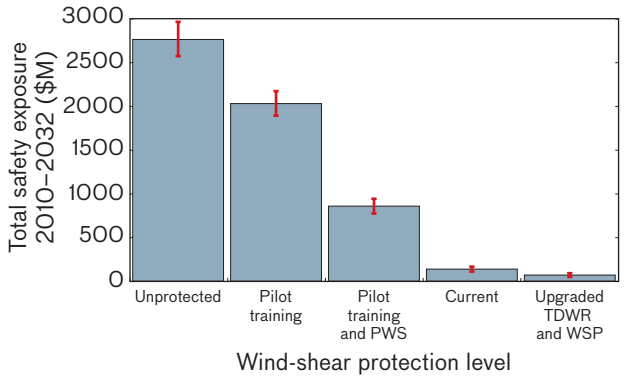


**FIGURE 16.** The total annual safety-related financial exposure from wind-shear accidents is dependent upon the type of protection applied (based on the current value of fiscal year 2008). The error bars show the range of values based on the minimum/maximum estimates of accident rates given in Table 5.

### Airborne Mitigation Systems

Onboard systems include both reactive and predictive wind-shear systems. These systems are not routinely available on general-aviation or Part 135/7 aircraft. Predictive systems are available on approximately 63% of the air carrier fleet, and for this analysis we assume that those aircraft are randomly distributed throughout the country. While outside the scope of this study, variability in equipped aircraft between airports could impact the financial exposure of individual airports. As shown in Figure 16, the overall reduction in safety exposure from 2010 to 2032 relative to pilot training estimates is $1.1 billion or 56% ($109 million annually). The combined reduction from both pilot training and airborne systems relative to unprotected airspace is $1.9 billion or 68% ($178 million annually). This estimate assumes that the equipage rate stays constant throughout the period. If the equipage rate were 100% for air carriers, the safety exposure would be reduced by nearly $2.5 billion or a 91% reduction in safety liability ($240 million annually). Figure 17 shows the resultant remaining safety-related financial exposure for each class of airport, which is calculated on the basis of a NAS protected by both pilot training and PWS. These figures represent the baseline for comparisons of current and alternative ground-based wind-shear systems.

### Baseline Ground-Based Coverage

The current constellation of ground-based wind-shear protection systems comprises four configurations: TDWR, TDWR + LLWAS, WSP, and LLWAS. For the TDWR and WSP systems, upgrades to the algorithms and processors are already making their way through the system [18]. The current configuration, without upgrades, reduces safety-related wind-shear exposure by 84% ($752M) over that of pilot training and PWS, and results in an overall reduction from an unprotected NAS of 95% ($2.63B). System upgrades reduce the safety exposure at WSP sites by an additional $4.3M and by $56.1M at TDWR sites.

The remaining safety exposure in the system of about $160M from 2010 to 2032 roughly equates to one to two major air carrier accidents for the entire NAS over the 22-year period. About 47% of that safety exposure lies in the hundreds of smaller airports that were outside of the 161 airports included in this study. Individually, however, the hundreds of small airports that make up those outside operations have extremely low financial exposure, making investments in protection systems uneconomical.

Delay savings because of wind-shift prediction and planning from gustfront detection are significant for ground-based systems. The total estimated delay savings accrued from the upgrade of TDWR and WSP relative to the current baseline are estimated at $40 million over the 2010–32 life cycle. The safety and delay savings for the current and upgraded ground-based wind-shear detection systems is shown in Figure 18. Figure 19 shows the breakdown of safety and delay savings for the top 50 highest-benefit sites. The TDWR upgrade includes enhancements to reduce range-aliased obscuration of the interest region, allowing more wind shears and gustfronts to be

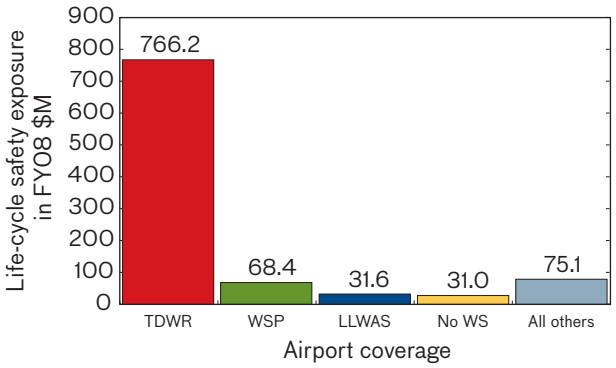


**FIGURE 17.** The total life-cycle safety-related financial exposure from wind-shear accidents, based on a National Airspace System protected by pilot training and airborne PWS. This is the residual liability after implementing the various protection systems. The column No WS is for airports without any wind-shear detection system.

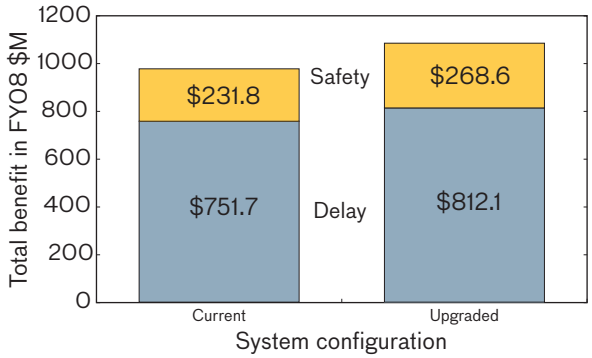


**FIGURE 18.** Safety-related savings (relative to coverage by pilot training and PWS only) and wind-shift delay benefits from gustfront detection and forecasting for current and TDWR/WSP upgraded system configuration (for 2010–2032) are slightly under and slightly over $1B.

detected. The WSP upgrade improves the maximum clutter suppression, enhancing WSP's ability to detect weaker wind shears and gustfronts in general.

### Airport-Specific Cost-Benefit Results

The final goal of the analysis is to determine which of the 20 wind-shear system alternatives is the optimal wind-shear solution for each site. An FAA-recommended analysis of Net Present Value (NPV) based on the system costs and overall safety and delay benefits for each site was used to make this assessment [17]. NPV is calculated by subtracting the cost of the alternative's development and/or operational costs from the estimated benefits of the system. Positive NPV means that a system's benefits outweigh its costs and that, therefore, safety improvements and/or delay reductions are worth implementing. This analysis also produces the best system configuration to optimize the safety and safety + delay without regard to cost at each site. The study results for each site show (1) the current wind-shear protection system, (2) the optimal (largest positive NPV) alternative based solely on safety benefits, (3) the optimal (largest positive NPV) alternative based on safety + delay, (4) the alternative that maximizes the safety benefit irrespective of cost, and (5) the alternative that maximizes the safety + delay benefit irrespective of cost.

In some cases, the optimal solution is "none," indicating that none of the alternatives were considered cost effective (NPV > 0). This does not mean that the alternative did not provide safety and/or delay benefits, only that the cost of operations was higher than those benefits.

In evaluating the various combinations of alternatives, most comparisons are made relative to the NAS as protected by pilot training and PWS or as protected by the upgraded ground-based system configuration, called "baseline" henceforth, although other comparisons may

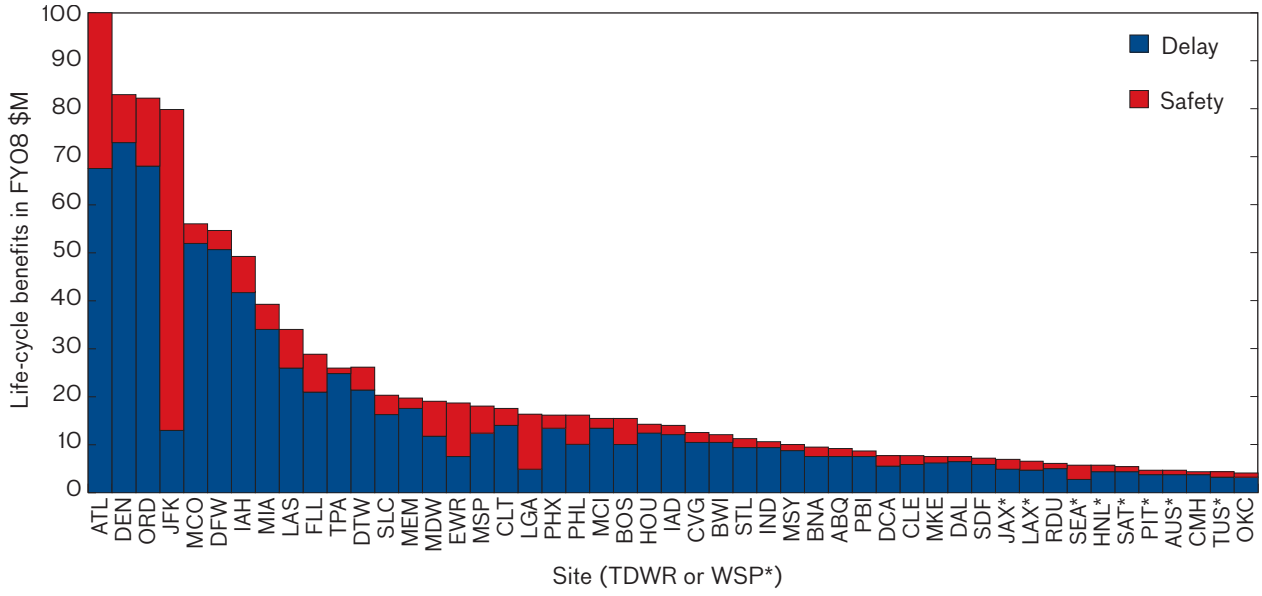


**FIGURE 19.** The life-cycle benefits of the top 50 sites in terms of total benefits (safety and delay) relative to the NAS as protected by pilot training and PWS for the upgraded baseline ground-based wind-shear system configuration (pilot training + PWS + current ground-based + planned upgrades). Delay benefits dominate in locations where there are multiple airports trying to use the same airspace (JFK-Kennedy, EWR-Newark, and LGA-LaGuardia in the New York City area, for example).

be made where appropriate. As noted above, the upgraded ground-based coverage yields a total safety-related benefit for the 161 study airports of $812 million and a wind-shift delay savings benefit of $269 million from 2010–32, or $77.1 and $25.5 million annually, respectively. While each optimal alternative yields an increase in the benefits relative to the upgraded baseline, the total increase in the benefits stream if every alternative listed were to be employed is approximately $76 million ($7.3 million annually), or roughly a 7% increase from the baseline benefits.

### Alternative System Assessment

As described above, the availability of some alternatives such as TDWR and WSP is limited by the current configuration. Therefore, it is instructive to examine the relative worth of system alternatives grouped by site type. The contingency Table 8 shows the number of times a particular wind-shear system alternative for safety savings was chosen as the optimal solution for each airport protection configuration. The numbers for safety and delay savings are similar. Alternatives that are not shown did not have any sites where they were the optimal system.

Looking strictly at the safety benefits of the system without implementation and operating costs allows us to examine the systems that could potentially provide the highest safety improvements at each site. Table 8 shows the individual site results for the best safety-improvement alternative at each site, but there are general trends that are summarized here. Figure 20 shows the ranking of alternative systems by changes in safety benefit for each grouping of current ground-based sites: TDWR, WSP, LLWAS, and unprotected. All alternatives are measured against the baseline configuration, so the entry for Upgraded will always show zero. Alternatives to the right of Upgraded provide increased safety improvements from the baseline and those to the left indicate reductions. In addition, for these safety charts, the top of the chart reflects the maximum safety benefit that could be achieved (zero accidents).

| OPTIMAL SYSTEM | CURRENT CONFIGURATION | | | | | |
|---|---|---|---|---|---|---|
| | TDWR AND LLWAS | TDWR | WSP | LLWAS | NO WS | TOTAL |
| TDWR | 1 | 12 | | | 5 | 18 |
| TDWR & LLWAS | 2 | | | | | 2 |
| TDWR & NEXRAD | | 1 | | | | 1 |
| TDWR, NEXRAD, and LLWAS | | | | | | 0 |
| TDWR & lidar | | 1 | | | | 1 |
| WSP | | | 14 | | | 14 |
| WSP & lidar | | | | | | 0 |
| LLWAS | 1 | | | 3 | 1 | 5 |
| NEXRAD & LLWAS | 3 | | | | | 3 |
| NEXRAD | 2 | 20 | 12 | 13 | 8 | 55 |
| None | | 3 | 9 | 24 | 26 | 62 |
| Total | 9 | 37 | 35 | 40 | 40 | 161 |

**TABLE 8.** The current configurations of ground-based sensors at some locations lend themselves to specific cost-effective optimizations. The blank spaces indicate those sites where the alternative optimal system is not economically viable when compared to the current configurations. No WS indicates no current wind-shear sensing system.

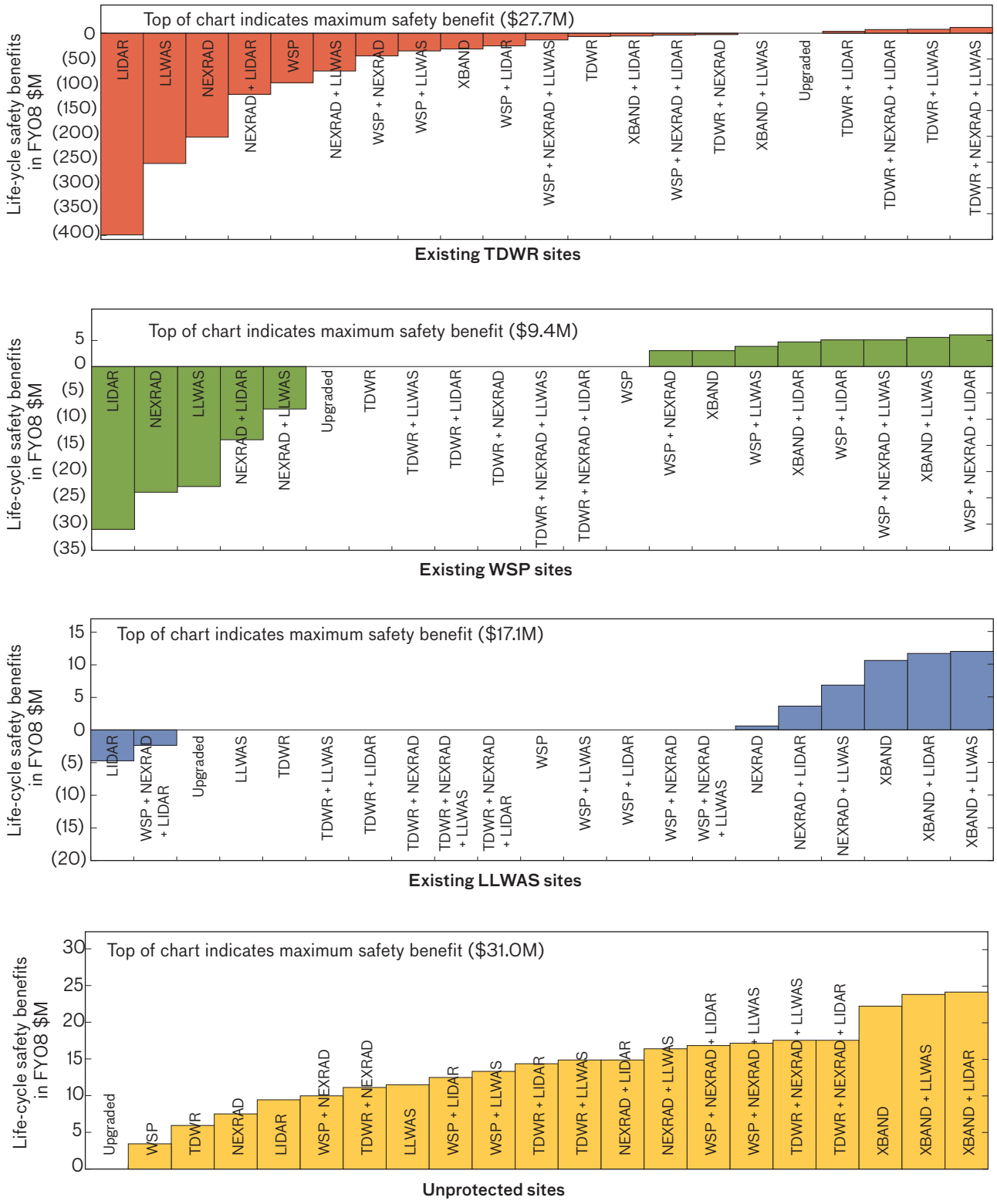


**FIGURE 20.** Annual benefit gain or loss relative to the upgraded baseline for alternatives being deployed at all (a) TDWR and TDWR-LLWAS study airports, (b) at all WSP study airports, (c) at all LLWAS study airports, and (d) at all study airports with no current ground-based wind-shear system. The baseline zero gain or loss is labeled "upgraded" in each chart. Note that there are very few options to improve TDWR sites, whereas all options for the unprotected sites show a life-cycle safety benefit.

As Figure 20 shows, the TDWR sites have few options that can provide overall safety improvements. However, integrating sensors to the TDWR is beneficial over the current system and all the positive options include the TDWR as a base sensor. Like TDWR, the rankings for WSP sites show that adding a sensor to complement the WSP is beneficial. But, in addition, X-band combinations also yield improved safety benefits. LLWAS sites have far fewer options because no TDWR or WSP radars are collocated with these sites. However, NEXRAD-based systems provide significant safety benefits and on-airport X-band weather radars are by far the best alternative.

Finally, for unprotected sites, shown at the bottom of Figure 20, every alternative shows some benefit. TDWR offers some benefits to this class of site as five unprotected sites are near enough to an existing TDWR to be partially covered if upgrades were made for processing and displays. WSP also has coverage through the potential to upgrade existing ASR-9s at some additional sites. NEXRAD-based systems with LLWAS or LIDAR gain almost half of the remaining potential safety benefit. X-band combinations are again the best performers for these unprotected sites, but that is primarily because the system is available at all sites.

**TDWR System Alternatives**

Because the TDWR radar was designed and sited specifically for wind-shear detection, it is generally the best or next-best alternative at the sites where it is installed. No new TDWR installations were considered for this analysis. When one is comparing TDWR (or any other alternatives) to the baseline, it should be noted that nine TDWR locations are integrated with LLWAS-NE installations and these are all high-benefit sites. Therefore, alternatives such as TDWR + NEXRAD show a loss relative to the baseline because of the loss of the LLWAS integration at those high-value sites.

WSP is one potential alternative to the existing TDWR installations; however, in all cases, WSP performance would result in a performance degradation compared to the TDWR. Replacing all 45 TDWR or TDWR-LLWAS installations with WSP or WSP-LLWAS configurations, respectively, would result in a loss of $179 million in total life-cycle safety and delay benefits ($17 million annually).

A potential benefit exists at five unprotected study airports that are close enough to be covered by existing TDWR installations. All of these airports currently have no ground-based coverage and the total added benefit would be $8.79 million. No TDWRs are close enough to LLWAS-only sites to provide wind-shear benefits.

**NEXRAD System Alternatives**

NEXRAD is an attractive alternative to other radar-based systems as it is a multiagency radar (Department of Defense, National Weather Service, FAA), and because of that, the expected additional costs for adding operational microburst and gustfront capability are much smaller than for competing systems. In fact, gustfront-detection algorithms are already part of the NEXRAD suite of algorithms. However, the radar siting is primarily based on coverage of population centers and not on airport locations. Effectivity estimates from the Lincoln Laboratory simulation study indicate that, despite location issues, a significant number of sites are covered adequately. NEXRAD provides coverage for wind shear at 74 of the 161 airports studied, and, at 53 of those sites, it achieves wind-shear probability of detections (PODs) greater than 90%. In addition, about one-third of the high-POD sites are non-WSP and/or non-TDWR sites.

One caution should be noted in interpreting these results. TDWR and WSP simulation results were compared against measured results from field studies, but NEXRAD has never been used for microburst detection. The effectivity simulation attempts to measure the potential for a system to detect microbursts and gustfronts on the basis of several metrics of wind-shear characteristics (wet/dry frequency, outflow depth, strength, etc.). The NEXRAD system, with combined wider beamwidths and longer distance, may be more sensitive to some of these characteristics than either TDWR or WSP. In addition, the NEXRAD revisits the surface, at most, once every four minutes, while TDWR does so every minute. For a NEXRAD system to be beneficial, it would most likely need to be modified to scan every minute.

However, sites with high PODs combined with the relatively inexpensive implementation costs overwhelmingly have NEXRAD-based alternatives as their optimal choices. A total of 63 airports have NEXRAD or NEXRAD + LLWAS as the optimal choice (three additional sites recommend NEXRAD in addition to TDWR).

### X-band Alternatives

The X-band radar and alternatives that combine with it are routinely the best-performing alternative at almost all sites. Certainly that is true at the LLWAS and unprotected sites for which TDWR and WSP alternatives were not even considered. But, even in high-value airports, this radar scored consistently high. Indeed, at 61 sites, X-band-based alternatives are chosen for highest safety coverage. That number increases to 77 sites if both safety and delay are considered.

However, the X-band radar is not a finished system, and implementation costs are estimated to be the highest of all alternatives. Because of this, no X-band system is chosen as an optimal system at any site. In addition, actual performance (many of the radar parameters were based on theoretical design) may be highly variable, and there may also be issues related to radar placement, especially at congested airports.

### LLWAS and Lidar Alternatives

No sites showed positive NPV benefits from implementation of an LLWAS or lidar system as a stand-alone system. However, both were sometimes beneficial in increasing safety coverage when used as a complementary system to radar coverage. In particular, lidar combinations were seen as an improvement at Las Vegas, Nevada, and Phoenix, Arizona. LLWAS benefits were confined to high-value sites such as Atlanta, Georgia, and Miami, Florida, where high traffic volumes and severe exposure to wind shear made even marginal increases in safety/delay very valuable.

## Future Work

The work done here represents the first retrospective on how well the research community did at significantly reducing the impact of wind-shear on aviation. The 1994 FAA report that formed the basis of the final investment decision for the TDWR estimated that there would be a better than 90% reduction in accident rates if the recommendations of the report were implemented. By our measures, the rate of wind-shear-related accidents dropped some 93% from 1985 to now. The total costs of those accidents dropped even more dramatically by 97%, likely because of improvements in aircraft technology and the heightened awareness of pilots who were warned by ground-based systems that they were entering known wind-shear situations.

But, the report does more than confirm the good work of researchers and private industry; it forms a basis for future investment and research decisions in the years to come. The wind-shear exposure maps provide the capability to know the risk factors at any location whether it be an airport or hot-air-balloon facility. The mitigation modeling methods can be used to incorporate new crash incidents with old to refine estimates of sparse raw accident-rate data. The ground-based detection modeling allows for researchers to evaluate and compare both changes in existing systems as well as the impact of new sensors. Finally, the end-to-end capability to incorporate not only safety and delay considerations but also cost issues when evaluating investments is a new capability for the weather-sensing community.

In fact, the components of this work have already been utilized to evaluate site alternatives for the TDWR serving JFK International airport in New York City, which must move from its current location in the next decade [19]. The FAA's NEXRAD office has funded a research study to understand how to implement wind-shear algorithms into their standard suite of algorithms. Finally, the FAA is utilizing the outline of this report to assist in the reorganization of its wind-shear protection division. ■

### REFERENCES


1. T.T. Fujita, *The Downbursts: Microbursts and Macrobursts,* Chicago: University of Chicago Press, 1985.
2. M.M. Wolfson, R.L. Delanoy, B.E. Forman, R.G. Hallowell, M.L. Pawlak, and P.D. Smith, "Automated microburst wind-shear prediction," *Linc. Lab. J.*, vol. 7, no. 2, 1994, pp. 399–426.
3. M.M. Wolfson, D. Klingle-Wilson, M. Donovan, J. Cullen, L. Neilley, M. Liepins, R. Hallowell, J. DiStefano, D. Clark, M. Isaminger, P. Biron, and B.E. Forman, "Characteristics of thunderstorm-generated low altitude wind shear: a survey based on nationwide Terminal Doppler Weather Radar testbed measurements," *Proc. 29th IEEE Conf. on Decision and Control*, Honolulu, Hawaii, vol. 2, 1990, pp 682–688.
4. Flightsim Aviation FAA Federal Aviation Regulations, http://www.flightsimaviation.com/data/FARS/part_121-358.html
5. Martin Marietta, "Wind shear systems cost-benefit and deployment study: system engineering and integration contract for implementation of the National Airspace System plan," *ATC-92-1201*, Martin Marietta Air Traffic Systems, 1994.
6. J.Y.N. Cho, R.G. Hallowell, "Detection probability modeling for airport wind-shear sensors," *Project Report ATC-340*, Lexington, Mass.: MIT Lincoln Laboratory, 2008.
7. F.W. Wilson, and R.H. Gramzow, "The redesigned low level

wind shear alert system," *Preprints 4th Intl. Conf. Aviation Weather Systems*, Paris, France, 2010, pp. 370–375.
8. M.W. Michelson, W.W. Shrader, and J.G. Wieler, "Terminal Doppler Weather Radar," *Microwave J.*, vol. 33, no. 2, 1990, pp. 139–148.
9. M.E. Weber, and M.L. Stone, "Low altitude wind shear detection using airport surveillance radars," *IEEE Aerosp. Electron. Syst. Mag.*, vol. 10, no. 6, 1995, pp. 3–9.
10. W.D. Heiss, D.L. McGrew, and D. Sirmans, "NEXRAD: next generation weather radar (WSR-88D)," *Microwave J.*, vol. 33, no. 1, 1990, pp. 79–98.
11. P.W. Chan, C.M. Shun, and K.C. Wu, "Operational LIDAR-based system for automatic windshear alerting at the Hong Kong International Airport," *Preprint, 12th Conf. Aviation, Range, and Aerospace Meteorology, Amer. Meteor. Soc.*, Atlanta, Ga., 2006 (http://ams.confex.com/ams/pdfpapers/100601.pdf).
12. S.M. Hannon, "Pulsed Doppler lidar for terminal weather area monitoring of wind and wake hazards," *Preprints, 11th Conf. Aviation, Range, and Aerospace Meteorology, Amer. Meteor. Soc.*, Hyannis, Mass., 2004, p. 4.21 (http://ams.confex.com/ams/pdfpapers/87757.pdf).
13. F.W. Wilson, and R.E. Cole, "LLWAS II and LLWAS III performance evaluation," *Preprints, 5th Conf. Aviation Weather Systems, Amer. Meteor. Soc.*, Vienna, Va., 1993, pp. 204–208.
14. R.E. Cole, and R.F. Todd, "A comparative performance study of TDWR/LLWAS 3 integration algorithms for wind shear detection," *Preprints, Workshop on Wind shear and Wind Shear Alert Systems, Amer. Meteor. Soc.*, Oklahoma City, Okla., 1996, pp. 43–52.
15. Federal Aviation Administration, "Official terminal area forecast of aviation activity for US airports," (http://aspm.faa.gov/main/taf.asp).
16. GRA, Incorporated, "Economic values for FAA investment and regulatory decisions, A guide, Final Report," October 3, 2007, p. 96.
17. Federal Aviation Administration, "Revised department guidelines: treatment of the value of preventing fatalities and injuries in preparing economic analyses," 2008.
18. J.Y.N. Cho, G.R. Elkin, and N.G. Parker, "Enhanced radar data acquisition system and signal processing algorithm for the TDWR," *Preprints, 32nd Conf. Radar Meteorology, Ameri. Meteor. Soc.,* Albuquerque, N.M., 2005, P4R.8, (http://ams.confex.com/ams/pdfpapers/96018.pdf).
19. S. Huang, J.Y.N. Cho, M.F. Donovan, R.G. Hallowell, and R.S. Frankel, "Redeployment of the New York TDWR: Technical analysis of candidate sites and alternative wind shear sensors, *Project Report ATC-351*, Lexington, Mass.: MIT Lincoln Laboratory, 2009.

## ABOUT THE AUTHORS

**Robert G. Hallowell** is an associate staff member in the Weather Sensing Group. Since 1986, he has supported and led research efforts on microbursts for the TDWR program and on software development in the area of microburst prediction for the Integrated Terminal Weather System program and the convective weather forecast algorithm for the Corridor Integrated Weather System. He coauthored several patents that are utilized today by several private weather vendors to provide forecasts of thunderstorm movement. More recently, he has collaborated with other national laboratories to develop an automated road-weather-forecast system for winter maintenance operators. He received his bachelor's degree in meteorology from the University of Massachusetts, Lowell.

**John Y. N. Cho** is a technical staff member in the Weather Sensing Group. Before joining the Laboratory, he was a research scientist in the Department of Earth, Atmospheric, and Planetary Sciences at MIT, following a stint as a staff scientist at the National Astronomy and Ionosphere Center's Arecibo Observatory in Puerto Rico. He has also been a visiting scientist at the Leibniz Institute for Atmospheric Physics in Germany. Honors received include the National Science Foundation CEDAR Prize, the Union Radio-Scientifique Internationale Young Scientist Award, and NASA's Group Achievement Award. He has authored over forty refereed journal articles and holds bachelor's and master's degrees from Stanford University, and a doctorate from Cornell University, all in electrical engineering. He also served with the U.S. Peace Corps in Sierra Leone.